

Torsional Oscillator Studies of the Superfluidity of ^3He in Aerogel

H Alles^a, J J Kaplinsky^a P S Wootton^a
J D Reppy^{a,1} and J R Hook^a

^a*Schuster Laboratory, University of Manchester, Manchester, M13 9PL, U.K.*

Abstract

We have made simultaneous torsional oscillator and transverse NMR measurements (at $\sim 165\text{kHz}$) on ^3He contained within aerogels with nominal densities of 1% and 2% of solid glass. The superfluid transition is seen simultaneously by both techniques and occurs at a temperature which agrees semi-quantitatively with that expected for homogeneous isotropic pair-breaking scattering of ^3He atoms by strands of silica. Values obtained for the superfluid density ρ_s in the 2% sample are in reasonable agreement with those observed previously. Coupling of the torsional mode to a parasitic resonance prevented accurate determination of ρ_s for the 1% aerogel. We have identified other resonances coupling to the torsional oscillations as sound modes within the helium/aerogel medium.

Key words: Superfluid ^3He , aerogel, sound modes, torsional oscillator.

1 Introduction

The discovery of superfluidity of ^3He in low density aerogel glass in torsional oscillator experiments at Cornell University[1] and its subsequent investigation in NMR experiments at Northwestern University[2] raised many interesting questions; for example:

- Would the transition seen in the torsional oscillator be coincident with the onset of an NMR frequency shift?
- How many superfluid phases are there and what is the phase diagram?
- What is the nature of the pairing?

¹ present address: LASSP, Clark Hall, Cornell University, Ithaca, NY 14853, USA.

- Is it possible to explain theoretically the effect of the aerogel on the properties of the superfluid phase(s)?

In an attempt to address these questions we decided to perform simultaneous torsional oscillator and NMR experiments on the same sample.

In this paper we report the results of torsional oscillator measurements on aerogel samples with 1% and 2% of solid density. Analysis of the NMR data is still in progress so we do not report these results in detail here.

2 Experimental method

The aerogel was grown within a spherical glass container with outer and inner diameters of order 10 mm and 8 mm respectively as shown in Fig. 1. Two samples have been studied with nominal densities of 1% and 2% of that of solid glass. The ^3He entered the cell via a glass stem with an internal diameter of about 1 mm. In the case of the 1% sample the spherical envelope was completely filled with aerogel but for the 2% sample a small region of bulk liquid was present near the stem as indicated in Fig. 1. The glass stem was glued to a beryllium copper capillary with stycast 2850 GT epoxy[3]; the capillary acted as the fill line and also provided the torsion rod for torsional oscillations of the cell. The torsional oscillations were excited and detected electrostatically using electrodes mounted on the low pass vibration filter shown in Fig. 1. The vibration frequencies for the 1% and 2% samples were of order 850 Hz and 970 Hz respectively. A two-phase lockin amplifier was used to measure the output from the detection electrode; from the in-phase and quadrature signals the resonant frequency and bandwidth of the oscillator were determined. Computer control of the driving frequency and voltage ensured that the oscillator was driven close to its resonant frequency and at a user-specified amplitude[4].

We were also able to simultaneously make transverse NMR measurements on the ^3He at frequencies up to about 200 kHz; a full account of the NMR experiments will be given later. Temperature was measured using an LCMN thermometer mounted in a separate tower. The LCMN was calibrated against the transition temperature of bulk ^3He [5]; the superfluid transition of the ^3He in the thermometer was identified from the change in warming rate of the LCMN. As we were able to detect the bulk superfluid transition in both the thermometer and the glass sphere we were able to monitor and correct for the small temperature differences between thermometer and aerogel.

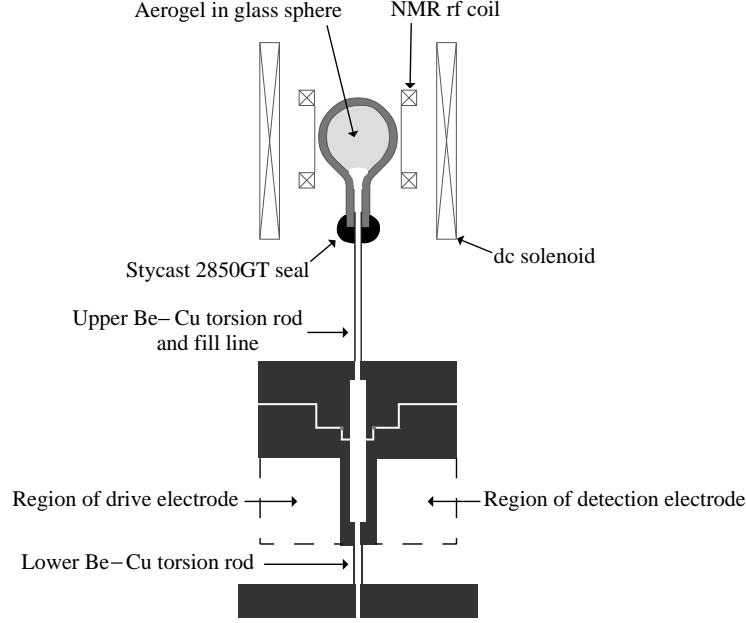


Fig. 1. Schematic diagram of the experimental setup. The large moment of inertia of the demountable Be-Cu cylinder between the upper and lower torsion rods together with the lower torsion rod provides a low pass filter preventing high frequency vibrational noise reaching the torsional oscillator. The drive and detection electrodes are situated underneath the Be-Cu cylinder in the regions shown, thus avoiding the need to attach electrodes to the glass sphere and also allowing the use of electrodes of larger area.

3 Superfluid transition temperature

Fig. 2 shows the superfluid transition temperature T_{ca} of the ^3He in the aerogel at various pressures relative to the superfluid transition temperature T_c of bulk ^3He . The values of T_{ca} are plotted as functions of the bulk coherence length which we define as

$$\xi_0 = \frac{\hbar v_F}{2\pi k_B T_c}. \quad (1)$$

For the 2% aerogel the values of T_{ca} were obtained from the torsional oscillator frequency measurements as described in Sec. 4. For the 1% aerogel the values of T_{ca} were those below which a shift in NMR frequency from the Larmor value was observed; as explained in Sec. 5. it was not possible to use the torsional oscillator frequency to identify the transition reliably at all pressures.

To the extent that the aerogel behaves like a dilute impurity which subjects the ^3He superfluid to isotropic pair breaking scattering the reduction in transition

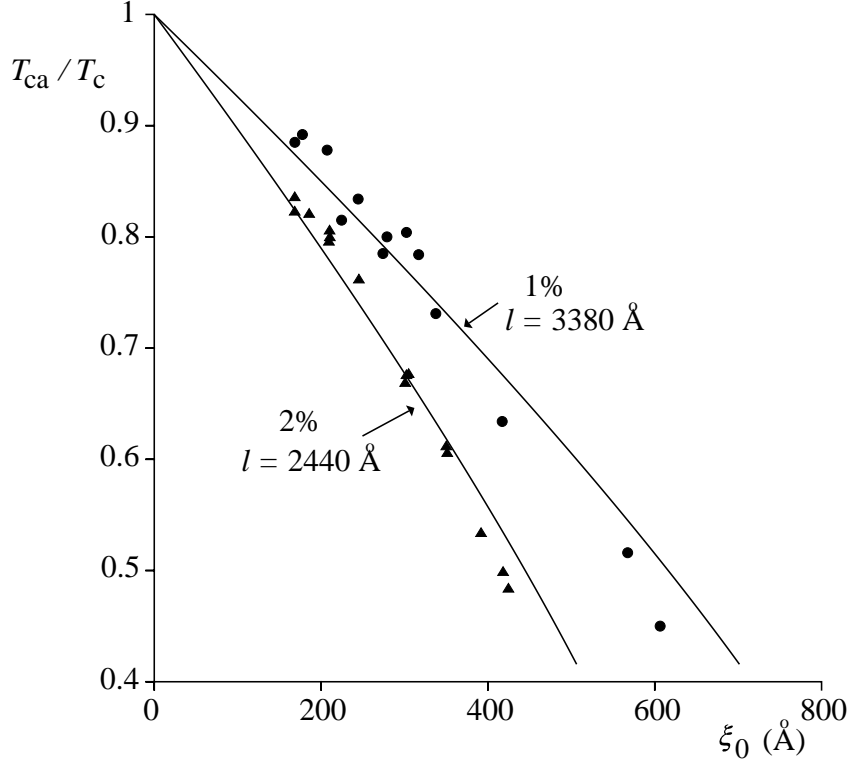


Fig. 2. Superfluid transition temperature for ^3He in aerogel at various pressures. The circles and triangles are for 1% and 2% aerogel respectively. The theoretical curves are fits of the data to Eq. (2) using values of the mean free path l of 3380 Å and 2440 Å for the 1% and 2% aerogel respectively.

temperature should be given by the following implicit equation[6,7]

$$\ln\left(\frac{T_{\text{ca}}}{T_c}\right) = \psi\left(\frac{1}{2}\right) - \psi\left(\frac{1}{2} + \frac{\xi_0 T_c}{l T_{\text{ca}}}\right), \quad (2)$$

where $\psi(x)$ is the digamma function and l is the mean free path associated with the scattering. We have adjusted l to obtain the best possible fits to the experimental data; the values required were 3380 Å and 2440 Å for the 1% and 2% aerogel respectively. As has also been observed in other experiments[7,8], there is a small but systematic difference between the observed pressure dependence and that predicted by Eq. (2) although this could be evidence for a small pressure dependence of l . The values of l are close to those obtained in a naive calculation for collisions of ^3He atoms with silica strands of diameter 3 nm[7]. Such a calculation predicts that l should be inversely proportional to the aerogel density; that our fitted values of l differ by less than a factor of two probably indicates that the real densities of our aerogel samples differ somewhat from their nominal values. We note that other measurements of T_{ca} for aerogels with nominal density 2% of solid show considerable variation. Our

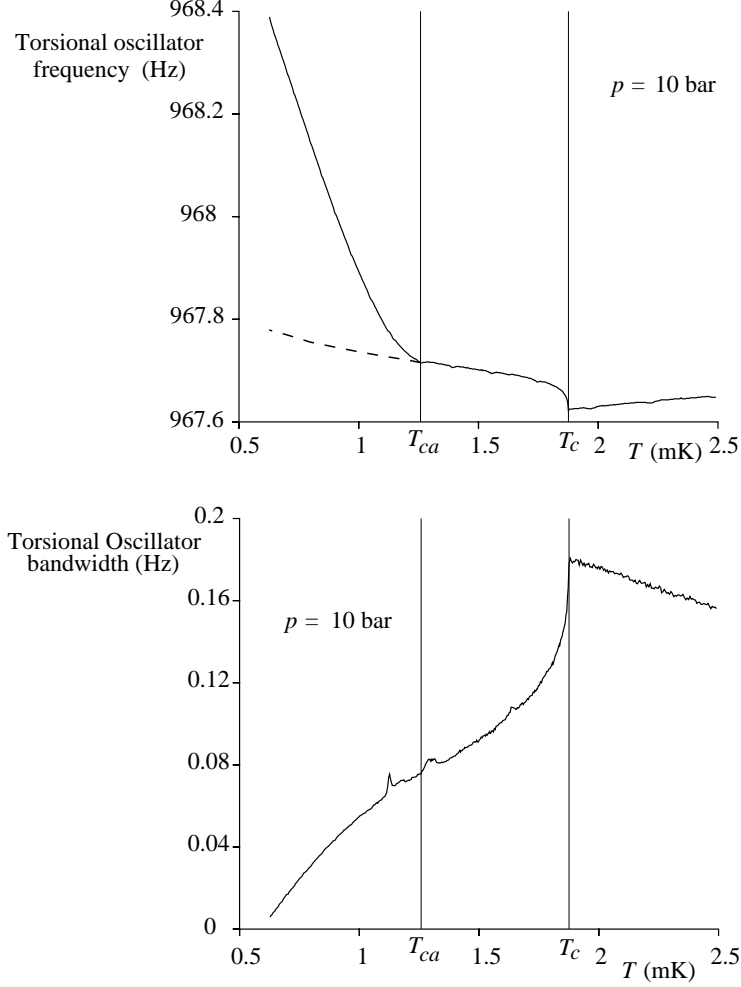


Fig. 3. Resonant frequency and bandwidth of the torsional oscillator as a function of temperature at 10 bar pressure for 2% aerogel.

values of T_{ca} lie between those of Ref. [1] and those of Refs. [2] and [9].

One important deduction that can be made from the success of Eq. (2) in describing the depression of the superfluid transition is that this indicates that the Cooper pairing within the aerogel is of the same type as in bulk, namely p-wave.

4 Measurements for 2% aerogel

Fig. 3 shows measurements of bandwidth and resonant frequency of the torsional oscillator for 2% aerogel filled with ^3He at 10 bar pressure; the temperatures, T_c and T_{ca} , of the superfluid transitions of the small region of bulk ^3He and of the ^3He in the aerogel are indicated. Above T_{ca} the temperature

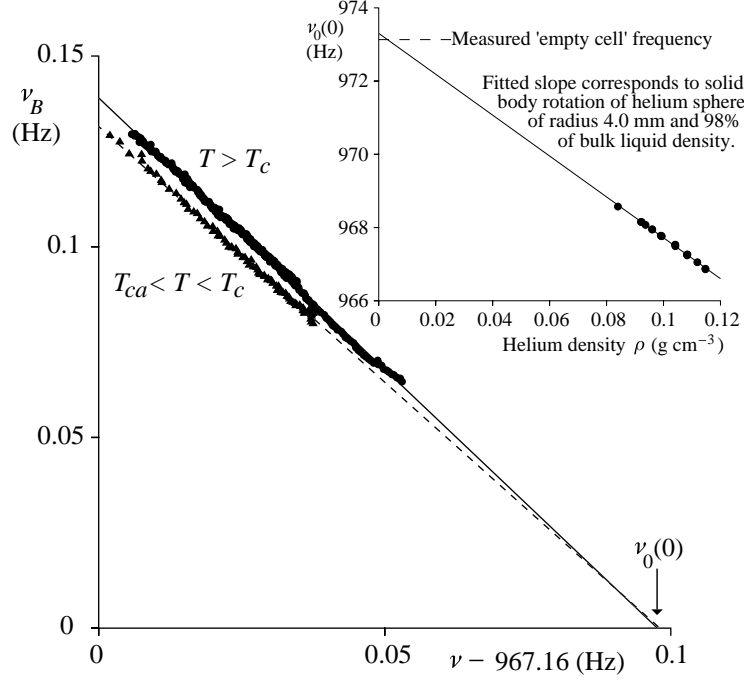


Fig. 4. Bandwidth versus resonant frequency of the torsional oscillator for $T > T_c$ (filled circles) and for $T > T_{ca}$ (filled triangles). Extrapolation of the linear relation to zero bandwidth as shown enables the frequency $\nu_0(0)$ to be determined. Values of $\nu_0(T)$ for $T < T_{ca}$ were obtained by using the measured bandwidth at T and the extrapolation of the $T > T_{ca}$ data. The inset (top right) shows values of $\nu_0(0)$ as a function of ρ ; the straight line fit has an intercept which agrees with the empty cell frequency within experimental error.

dependence is associated entirely with the small region of bulk liquid; the aerogel and ^3He within it behave as though rigidly locked to the motion of the oscillator. The increase in resonant frequency below T_{ca} signifies the decoupling of the superfluid fraction within the aerogel from the motion of the oscillator. The superfluidity of the ^3He within the aerogel does not produce any additional dissipation; apart from the small peak in bandwidth just below T_{ca} and scarcely visible increments in dissipation even closer to T_{ca} , which are discussed further below, the dissipation is associated entirely with the bulk liquid region. There is no evidence that the oscillator frequency and bandwidth depend significantly on magnetic fields up to 51 Gauss, the value used in most of our NMR measurements.

To determine the reduced superfluid density ρ_s/ρ within the aerogel we use

$$\frac{\rho_s}{\rho} = \frac{\nu(T) - \nu_0(T)}{\nu_e - \nu_0(0)}, \quad (3)$$

where $\nu(T)$ is the measured resonant frequency at temperature T as indicated

by the solid line on Fig. 3, $\nu_0(T)$ is the frequency indicated by the dashed line that would be expected at temperature T in the absence of superfluidity in the aerogel and ν_e the measured frequency of the cell prior to filling with ^3He ; $\nu_0(0)$ is the frequency to be expected for the case where the ^3He within the aerogel is rigidly coupled to the motion of the oscillator but the bulk ^3He is completely decoupled. The value of $\nu_0(0)$ could be obtained from both the normal state data at sufficiently high temperatures and the data just above T_{ca} ; in both these cases the viscous penetration depth $\delta = \sqrt{2\eta/\rho_n\omega}$ is small compared to the size of the bulk liquid region leading to linear relations between bandwidth and resonant frequency as shown in Fig. 4. Extrapolation of these relationships to zero bandwidth ($\equiv \delta \rightarrow 0$) allows $\nu_0(0)$ to be determined. At all pressures the values obtained from the two extrapolations agreed within an experimental uncertainty of about 10 mHz. To obtain the value of $\nu_0(T)$ for $T < T_{\text{ca}}$ the extrapolation of the bandwidth vs frequency for the $T > T_{\text{ca}}$ data was used as shown by the dashed line on Fig. 4. Since the dissipation was unaffected by the superfluid transition within the aerogel the measured bandwidth at the temperature concerned allowed us to obtain a value for the ‘unshifted’ resonant frequency. This method ignores possible departures from hydrodynamic behaviour within the bulk region at low temperatures; since the variation of $\nu_0(T)$ with temperature is very weak (see the dashed line on Fig. 3), this is unlikely to lead to significant error. The values obtained for $\nu_0(0)$ at different pressures are shown in the inset on Fig. 4 as functions of the density ρ of bulk ^3He at the pressure concerned; the straight line through the data corresponds to that expected for rigid torsional oscillations of a sphere of diameter 4 mm and density 0.98ρ . The extrapolation of the line at $\rho = 0$ to a value close to the measured empty cell frequency confirms our belief that the aerogel in the 2% sample moves rigidly with the glass envelope.

Values of ρ_s/ρ at different pressures obtained using Eq.(3) are shown in Fig. 5. The behaviour is qualitatively similar to that observed by Porto and Parpia[1,8] also for aerogel of nominal 2% of solid density; the data from Ref. [8] at 29 bar are also shown on Fig. 5. The temperature dependence of ρ_s/ρ is very different to that of bulk ^3He . It rises more slowly as T decreases through T_{ca} and approaches a value substantially less than unity at the lowest temperatures; this latter feature is more apparent in the data of Ref. [8] than in our data. Our data share with that of Ref. [8] the character that close to T_{ca} the values of ρ_s/ρ at different pressures can be superimposed to a good approximation by a translation along the temperature axis. For $T/T_{\text{ca}} > 0.75$, ρ_s/ρ is well fitted by a temperature dependence

$$\frac{\rho_s}{\rho} = A \left(1 - \frac{T}{T_{\text{ca}}}\right)^b. \quad (4)$$

An example of such a fit is shown in Fig. 6. The values of the exponent b at

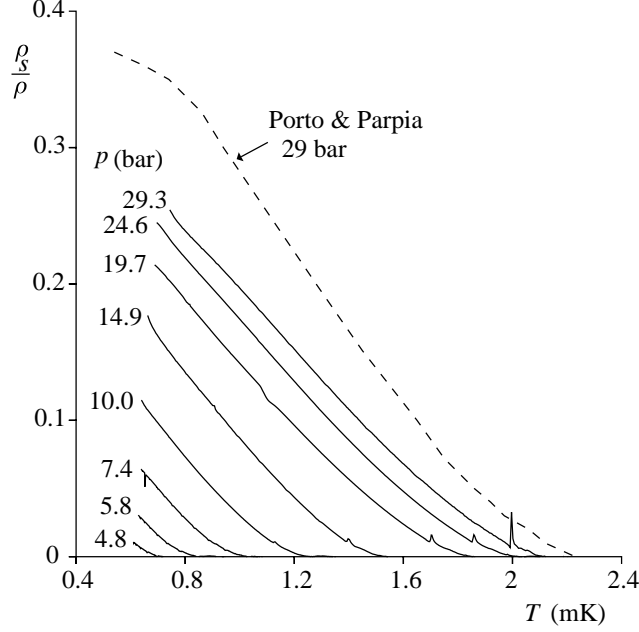


Fig. 5. Temperature dependence of ρ_s/ρ for 2% aerogel at the pressures indicated. The data of Porto and Parpia at 29 bar are shown by the dashed line.

different pressures are given in Fig. 7. Fits to the bulk superfluid density over the same range of reduced temperatures do not fit Eq. (4) well near T_c (where the correct limiting behaviour is $\rho_s/\rho \propto (1 - T/T_c)$) and produce significantly smaller values of $b \sim 1.25 - 1.30$. We note that Porto and Parpia obtained somewhat smaller values of b than ours from logarithmic fits ($\ln(\rho_s/\rho)$ vs $\ln(1 - T/T_{ca})$); also their values of b increased with increasing pressure. We used our fits to Eq. (4) as an objective way of determining the values of T_{ca} for the 2% aerogel; this proved to be a more accurate way than from the NMR frequency shift data. There is no evidence for a systematic difference between the transition temperatures observed by the two experimental methods as can be seen from Fig. 8 which compares NMR frequency shift data with the value of T_{ca} obtained from the torsional oscillator.

Finally in this section we discuss the peak in bandwidth which can be seen just below T_{ca} on Fig. 3. This peak was seen at all pressures above 7 bar but was largest at high pressures where a corresponding feature in the resonant frequency produced the small glitches in ρ_s/ρ on Fig. 5. The occurrence of the peak just below T_{ca} suggests a mode crossing of the torsional oscillator frequency with an internal mode of oscillation of the cell which has a frequency increasing from zero as ρ_s becomes finite within the aerogel. A second smaller peak in dissipation was observed even closer to T_{ca} ; there was evidence also for small additional dissipation between this second peak and T_{ca} . These observations suggest the existence of several internal modes such as might be associated with sound waves in the aerogel.

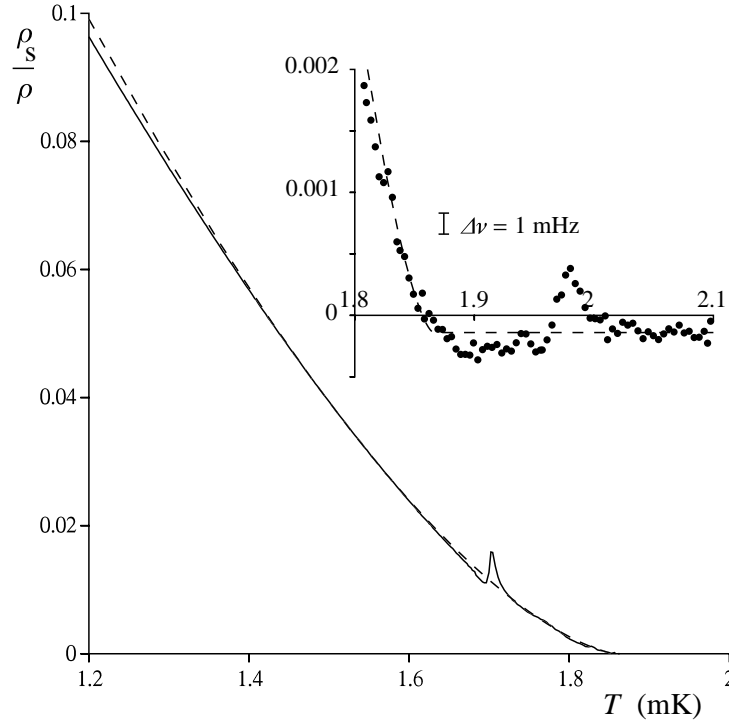


Fig. 6. Fit of ρ_s/ρ to Eq. (4) at 19.7 bar. The inset shows the behaviour close to T_{ca} ; the apparent value of a small negative ρ_s/ρ at $T > T_{ca}$ indicates a small error in the value of $\nu_0(T)$ used in the determination of ρ_s/ρ through Eq. (3). In both figures the fitted curve is shown with a dashed line.

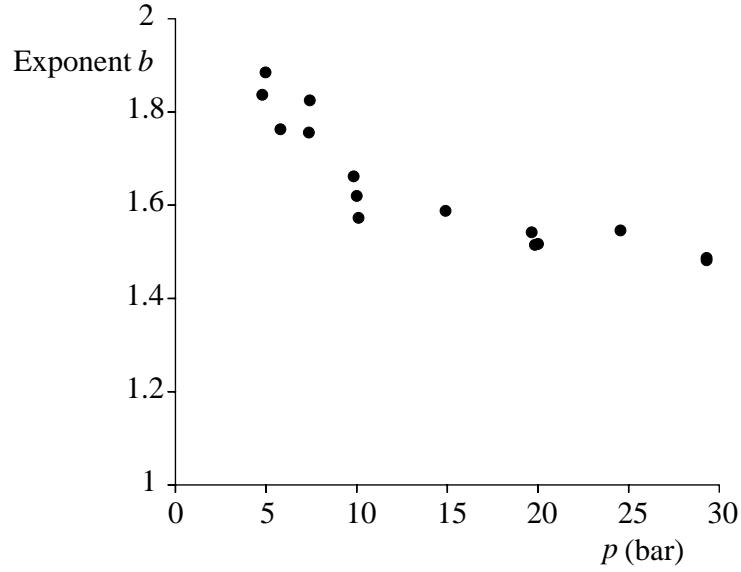


Fig. 7. Values of the exponent b giving the temperature dependence of ρ_s near T_c .

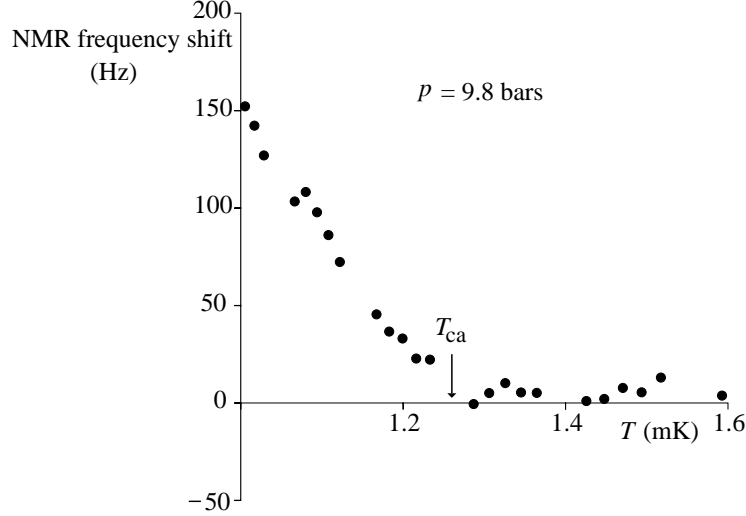


Fig. 8. NMR frequency shift as a function of temperature. The value of T_{ca} indicated was obtained from the torsional oscillator measurements.

Following McKenna et al[10], we assume that the normal fluid is rigidly locked to the aerogel. The sound speeds, c , are then the roots of the equation

$$c^4 - c^2(c_1^2 + c_2^2) + c_1^2 c_2^2 + \frac{\rho_a}{\rho_n}(c^2 - c_a^2)(c^2 - c_4^2) = 0, \quad (5)$$

where c_a is the speed of sound in the aerogel in the absence of the ^3He and c_1 , c_2 and c_4 are the speeds of first, second and fourth sound respectively. In ^3He , c_2 is very small and can be set to zero in Eq. (5). One of the roots of Eq. (5) goes to zero as $\rho_s \rightarrow 0$ and the sound modes in a sphere of radius a associated with this root are calculated in appendix A. The two lowest modes occur at angular frequencies $2.082c/a$ and $3.342c/a$ and lead to mode crossings with the torsional oscillator frequency at values of ρ_s/ρ given by the theoretical lines on Fig. 9. The fit with the experimental values was obtained by adjusting c_a ; the value used is 174 m s^{-1} . McKenna et al quote a value of $c_a \sim 100 \text{ m s}^{-1}$ for aerogel of 5% of solid density. Our value seems higher than might be expected for 2% aerogel since c_a is expected to decrease as the density of aerogel decreases[11]; it is possible that there will be variation between different samples of the same nominal density and also that c_a may vary with temperature. It is clear from inspection of Fig. 9 that there is a systematic difference in pressure dependence between the theoretical curves and experimental points. We have no explanation of this although we note that the experimental values at low pressures are not well determined because the peaks were very small and somewhat broader. We note that the existence of coupling between the torsional oscillations and the sound modes indicates that our experiment does not have perfect rotational symmetry about a vertical axis.

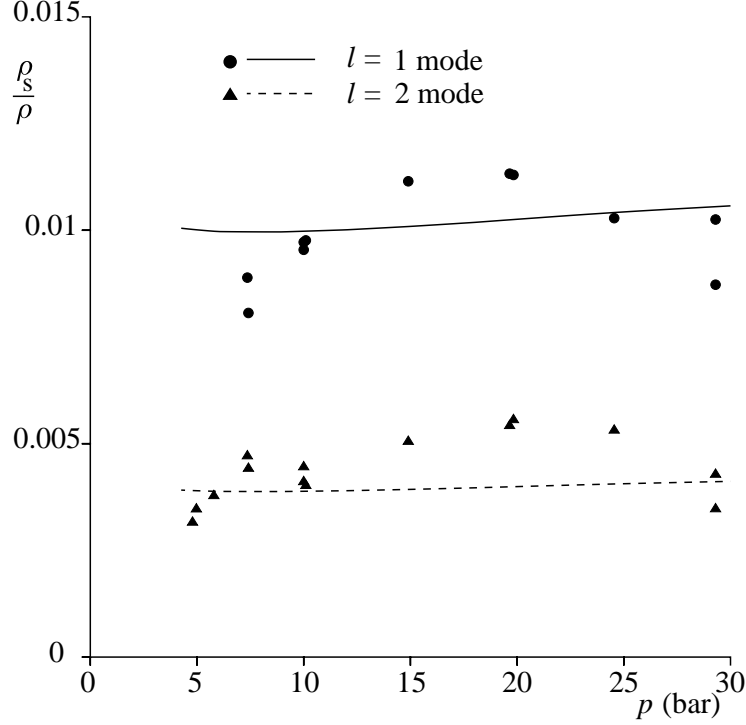


Fig. 9. Comparison between the experimental (circles and triangles) and theoretical (continuous and dashed line) values of ρ_s/ρ at which mode crossing of the torsional oscillator frequency with sound modes within the sphere occur.

We consider also the possibility that the intersecting mode is a Helmholtz resonance with pressure oscillations within the glass sphere producing oscillatory flow through the fill line. If our spherical container were filled only with ^3He then the geometry of our fill line is such that the Helmholtz frequency would always be more than a factor of two less than that of the torsional oscillator even when the superfluid fraction is 100%. The introduction of aerogel will decrease the frequency and hence the intersecting mode is not likely to be a Helmholtz resonance. There is a possibility that the sound modes discussed above could be modified by flow through the fill line. In appendix A we discuss a simple model which takes both the flow through the fill line and the spatial variation of pressure within the aerogel into account. The conclusion is that the fill line impedance is sufficiently high that flow through the fill line is unlikely to have had a significant effect on the sound mode frequencies.

5 Measurements for 1% aerogel

Fig. 10 shows the bandwidth and the resonant frequency as functions of temperature at 15.0 bar pressure for the 1% aerogel. The bulk superfluid transition is clearly seen in both the amplitude and bandwidth despite the absence of a

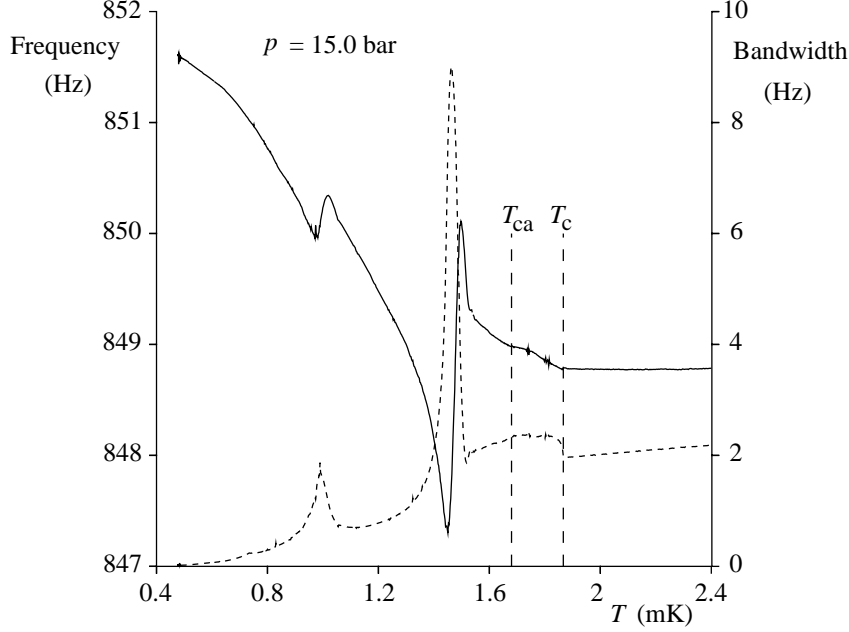


Fig. 10. Resonant frequency (continuous line) and bandwidth (dashed line) of the torsional oscillator at 15 bar pressure for the 1% aerogel.

macroscopic bulk superfluid region inside the sphere. The superfluid transition in the aerogel as determined from the NMR frequency shift is indicated and corresponds to an upturn in the resonant frequency with decreasing temperature just as for the 2% aerogel (Fig. 3). However, just below T_{ca} , the behaviour of the torsional oscillator is dominated by coupling to another resonant mode. We do not believe that this parasitic mode is a sound mode like those observed for the 2% aerogel. Indeed it may not be associated uniquely with the onset of superfluidity of the ^3He in the aerogel since at low pressures the coupling to this mode appears to be evident above T_{ca} ; it is this coupling above T_{ca} which prevented identification of T_{ca} from the torsional oscillator data at low pressures. The large magnitude of the coupling between the mode and the torsional oscillations together with the large bandwidth of the torsional oscillator at all temperatures in comparison with the 2% data suggest that significant shear motions of the 1% aerogel are being excited. Further evidence for this is the apparent discontinuity in the ‘background’ frequency of the torsional oscillator associated with the mode crossing. This possible discontinuity prevents the deduction of reliable values of superfluid density for the 1% aerogel at lower temperatures although we are currently searching for a theoretical description of the intersecting mode which might make this possible.

The smaller intersecting resonance which can be seen at lower temperatures on Fig. 10 is we believe due to a sound mode like those observed for the 2% aerogel. If we ignore the apparent discontinuity in the background frequency of the torsional oscillator mentioned in the previous paragraph we can estimate

a value of ρ_s at which this second resonance occurs and then by proceeding as for the 2% aerogel we can estimate the speed of sound c_a in the 1% aerogel. The value obtained is 55 m s^{-1} which, in view of our neglect of a possible background frequency discontinuity, must be regarded as an upper limit; the value is less than that for the 2% aerogel as would be expected.

For the 1% aerogel we investigated the effect of the addition of small quantities of ^4He on the torsional oscillator. About 3% of ^4He was sufficient to replace the solid He layer on the aerogel surfaces as indicated by the absence of a Curie-Weiss contribution to the NMR signal strength[2]. The addition of ^4He caused a dramatic reduction in the size of the parasitic resonances and of the oscillator bandwidth at higher temperatures; coupling to the intersecting resonances was almost completely absent at high pressures. We do not have any explanation for this observation. Although the parasitic resonances were absent we were still unable to determine the superfluid density within the aerogel because the addition of the ^4He also introduced a large thermal boundary resistance between the LCMN and the ^3He which preventing us from measuring the temperature.

6 Conclusions

In this concluding section we return briefly to the questions posed in our introduction. Our experiments show that the superfluid transition of ^3He in aerogel as indicated by the appearance of a finite superfluid density coincides with the onset of a shift in the NMR frequency. Our torsional oscillator measurements provide no evidence for more than one superfluid phase and do not identify the nature of the pairing although our observation that the measured superfluid density is independent of applied magnetic fields up to about 50 Gauss might be interpreted as implying that the superfluid phase is one with an isotropic superfluid density. We are hoping that the completion of our analysis of our NMR measurements will provide further information on the questions of the number of phases and the nature of the pairing. The fact that we measure two different properties on the same sample of aerogel should provide a stringent test for theories purporting to explain the effect of aerogel on the properties of the superfluid.

Acknowledgements

We have benefitted greatly from discussions with Henry Hall. We are grateful to Norbert Mulders, Jongsoo Yoon and Moses Chan for providing the aerogel specimens used in our experiments. This work was supported by EPSRC

through Research Grants GR/K59835 and GR/K58234, and by the award of Research Studentships to JJK and PSW.

References

- [1] J. V. Porto and J. M. Parpia, Phys. Rev. Lett. **74**, 4667 (1995).
- [2] D. T. Sprague, T. M. Haard, J. B. Kycia, M. R. Rand, Y. Lee, P. J. Hamot and W. P. Halperin, Phys. Rev. Lett. **75**, 661 (1995).
- [3] Emerson and Cumming of Canton MA 020221, USA.
- [4] J. R. Hook, E. Faraj, S. G. Gould and H. E. Hall, J. Low Temp. Phys. **74**, 45 (1989).
- [5] D. S. Greywall, Phys. Rev. B **33**, 7520 (1986).
- [6] L P Gor'kov, ZETF **39**, 1781 (1960), Translation Soviet Phys. JETP **10**, 593 (1960).
- [7] E. V. Thuneberg, S. K. Yip, M Fogelström and J. A. Sauls, Phys. Rev. Lett. **80**, 2861 (1998).
- [8] J. V. Porto and J. M. Parpia, Czech. J. Phys. **46**, 2981 (1996).
- [9] K. Matsumoto, J. V. Porto, L. Pollack, E. N. Smith, T. L. Ho and J. M. Parpia, Phys. Rev. Lett. **79**, 253 (1997).
- [10] M. J. McKenna, T. Slaweki and J. D. Maynard, Phys. Rev. Lett. **66**, 1878 (1991).
- [11] J. Gross, G. W. Scherer, C. T. Alviso and R. W. Pekala, J. Non-Cryst. Solids **211**, 132 (1997).
- [12] M. Abramowitz and I. A. Stegun, *Handbook of Mathematical Functions* (Dover, New York 1965).
- [13] J. R. Hook, T.D.C. Bevan, A.J. Manninen, J.B. Cook, A.J. Armstrong and H.E. Hall, Physica B **210**, 251 (1995).

A Sound Modes and Helmholtz Resonance

We consider first the sound modes in a spherical cavity of radius a completely filled with aerogel containing ^3He . The small value of c_2 for ^3He means that the effect of temperature gradients within the cavity can be ignored and the equations of motion which describe the ^3He /aerogel combination are then[10]

$$\frac{\partial \rho}{\partial t} = -\nabla \cdot (\rho_s \mathbf{v}_s + \rho_n \mathbf{v}_n), \quad (\text{A.1})$$

$$\frac{\partial \mathbf{v}_s}{\partial t} = -\frac{1}{\rho} \nabla p, \quad (\text{A.2})$$

$$(\rho_a + \rho_n) \frac{\partial \mathbf{v}_n}{\partial t} = -\frac{\rho_n}{\rho} \nabla p - \nabla p_a, \quad (\text{A.3})$$

$$\frac{\partial \rho_a}{\partial t} = -\nabla \cdot (\rho_a \mathbf{v}_n), \quad (\text{A.4})$$

where ρ and ρ_a are the densities of helium and aerogel, p is the pressure acting on the helium and p_a is the pressure acting on the aerogel due to its elastic distortion; the motion of the aerogel and normal fluid are assumed to be locked together. Assuming that small variations in p and p_a are related to the corresponding densities by $\delta p = c_1^2 \delta \rho$ and $\delta p_a = c_a^2 \delta \rho_a$, we obtain from Eqs. (A.1) to (A.4) the following equation for small harmonic departures, $\delta \rho = \rho' \exp(i\omega t)$, of ρ from equilibrium

$$\nabla^4 \rho' + \omega^2 \left(\frac{1}{c_4^2} + \frac{1}{c_a^2} + \frac{\rho_n c_1^2}{\rho_a c_4^2 c_a^2} \right) \nabla^2 \rho' + \omega^4 \frac{(\rho_a + \rho_n)}{\rho_a c_4^2 c_a^2} \rho' = 0, \quad (\text{A.5})$$

where $c_4^2 = c_1^2 \rho_s / \rho$.

The solutions of Eq. (A.5) appropriate to our spherical geometry are of the form

$$\rho' = (A j_l(k_1 r) + B j_l(k_2 r)) Y_{lm}(\theta, \phi), \quad (\text{A.6})$$

where A and B are constants of integration, $j_l(z)$ is a spherical Bessel function, $Y_{lm}(\theta, \phi)$ is a spherical harmonic and we are using the notation of Abramowitz and Stegun[12]; the spherical Bessel functions $y_l(k_1 r)$ and $y_l(k_2 r)$ can be excluded from the solution because they diverge as $r \rightarrow 0$. The wave numbers k_1 and k_2 are the roots of

$$k^4 - \omega^2 k^2 \left(\frac{1}{c_4^2} + \frac{1}{c_a^2} + \frac{\rho_n c_1^2}{c \rho_a c_4^2 c_a^2} \right) + \omega^4 \frac{(\rho_a + \rho_n)}{\rho_a c_4^2 c_a^2} = 0, \quad (\text{A.7})$$

and are thus the wavenumbers associated with the sound speeds which satisfy Eq. (5) in the limit $c_2 \rightarrow 0$. The boundary conditions to be applied to the solution are that

$$\mathbf{v}_n \cdot \hat{\mathbf{r}} = \mathbf{v}_s \cdot \hat{\mathbf{r}} = 0 \quad \text{at} \quad r = a. \quad (\text{A.8})$$

The radial components of the \mathbf{v}_n and \mathbf{v}_s can be found for solution (A.6) by using Eqs. (A.1) to (A.4). Fortunately the boundary conditions produce no mix-

ing of the terms of different wavenumber and the modes occur at wavenumbers k ($= k_1$ or k_2) which satisfy

$$\left[\frac{d}{dr} j_l(kr) \right]_{r=a} = j_{l-1}(ka) - \frac{l+1}{ka} j_l(ka) = 0. \quad (\text{A.9})$$

The roots are thus characterised by two numbers n and l , where n specifies the number of radial nodes (excluding $r = 0$) in the variation of p . The values of ka (n, l) for the 7 lowest modes are 2.08157 (0,1), 3.34210 (0,2), 4.49341 (1,0), 4.51411 (0,3), 5.64670 (0,4), 5.94037 (1,1), 6.75645 (0,5). The two lowest modes with $n, l = 0, 1$ and $0, 2$ are the modes plotted in Fig. 9.

We now consider the possibility that the modes may be affected by flow through the fill line. Since a spherical cavity on the end of cylindrical fill line is difficult to calculate we consider instead a simplified model: a spherical cavity with a fill line entering at the centre. We take the end of the fill line to be surrounded by a small spherical region of bulk liquid of radius b . Only modes of spherical symmetry will have a pressure variation at the centre of the sphere. For these modes the general solution of Eq. (A.5) is

$$\rho' = (A_1 j_0(k_1 r) + B_1 y_0(k_1 r) + A_2 j_0(k_2 r) + B_2 y_0(k_2 r)). \quad (\text{A.10})$$

Because of the small region of bulk helium and the fill line at the centre of the sphere it is no longer possible to ignore the spherical Bessel function $y_0(z) = -\cos(z)/z$ which diverges as $z \rightarrow 0$. The boundary conditions to be applied at $r = a$ are Eqs. (A.8) as before and at the boundary of the bulk liquid region, $r = b$, we require that the variations of p_a should vanish and that the ratio of pressure variation $\delta p = p' \exp(i\omega t)$ to mass flow *out* of the aerogel $\dot{M} = -4\pi b^2(\rho_s v_s + \rho_n v_n)$ should be appropriate to the geometry of our fill line

$$\frac{\delta p(b)}{\dot{M}} = \frac{i\omega \rho L}{\rho_{sb} \sigma}, \quad (\text{A.11})$$

where L/σ is the ratio of fill line length to cross sectional area and ρ_{sb} is the superfluid density in the fill line. Eq. (A.11) follows from the equation of motion

$$\frac{\partial v_s}{\partial t} = i\omega v_s = \frac{\delta p(b)}{L\rho}, \quad (\text{A.12})$$

for the helium within the fill line. Note that we ignore the variation of pressure inside the sphere of radius b .

Applying the boundary conditions to the solution given by Eq. (A.10) leads to a rather complicated condition for determining the frequency of the spherically symmetric modes. The terms in Eq. (A.10) of wavenumbers k_1 and k_2 are no longer decoupled. We do not discuss the details here but report the general conclusion that the impedance of our fill line (L/σ) is sufficiently high that the modes under consideration are essentially sound modes with little flow through the fill line.